The Okavango giant mafic dyke swarm (NE Botswana): its structural significance within the Karoo Large Igneous Province

Bernard Le Gall[a,*], Gomotsang Tshoso[a], Jérôme Dyment[b], Ali Basira Kampunzu[c,⚰],
Fred Jourdan[d,e], Gilbert Féraud[d], Hervé Bertrand[e], Charly Aubourg[f], William Vétel[a]

[a]European Institute for Marine Studies CNRS-UMR 6538 Domaines Océaniques, UBO-IUEM Brest, France
[b]CNRS-UMR 7097, Laboratoire Géosciences Marines, IPG, Paris, France
[c]University of Botswana, Gaborone, Botswana
[d]CNRS-UMR 6526 Geosciences Azur, Nice-Sophia Antipolis, France
[e]CNRS-UMR 5570, ENS-UCB Lyon, France
[f]CNRS-UMR 7072, Cergy-Pontoise, France

Abstract

The structural organization of a giant mafic dyke swarm, the Okavango complex, in the northern Karoo Large Igneous Province (LIP) of NE Botswana is detailed. This N110°E-oriented dyke swarm extends for 1500 km with a maximum width of 100 km through Archaean basement terranes and Permo-Jurassic sedimentary sequences. The cornerstone of the study is the quantitative analysis of $N > 170$ (exposed) and $N > 420$ (detected by ground magnetics) dykes evidenced on a ca. 80-km-long section lying in crystalline host-rocks, at high-angle to the densest zone of the swarm (Shashe area). Individual dykes are generally sub-vertical and parallel to the entire swarm. Statistical analysis of width data indicates anomalous dyke frequency (few data < 5.0 m) and mean dyke thickness (high value of 17 m) with respect to values classically obtained from other giant swarms. Variations of mean dyke thicknesses from 17 (N110°E swarm) to 27 m (adjoining and coeval N70°E giant swarm) are assigned to the conditions hosting fracture networks dilated as either shear or pure extensional structures, respectively, in response to an inferred NNW–SSE extension. Both fracture patterns are regarded as inherited brittle basement fabrics associated with a previous (Proterozoic) dyking event. The Okavango N110°E dyke swarm is thus a polyphase intrusive system in which total dilation caused by Karoo dykes (estimated frequency of 87%) is 12.2% (6315 m of cumulative dyke width) throughout the 52-km-long projected Shashe section. Assuming that Karoo mafic dyke swarms in NE Botswana follow inherited Proterozoic fractures, as similarly applied for most of the nearly synchronous giant dyke complexes converging towards the Nuanetsi area, leads us to consider that the resulting triple junction-like dyke/fracture pattern is not a definitive proof for a deep mantle plume in the Karoo LIP.
© 2005 Elsevier Ltd. All rights reserved.

Keywords: Structure; Giant mafic dyke swarm; Okavango; Karoo Large Igneous Province; Botswana

1. Introduction

During the last two decades, igneous dyke swarms have received considerable attention in both intraplate Large Igneous Provinces (LIPs) and magmatic passive margins (White, 1992; Callot et al., 2001). This interest stems from the ability of dyke swarms to supply information on: (1) the relative timing of deformation vs. igneous activity; and (2) the amount of crustal extension during dyke emplacement. Therefore, dyke swarms can be kinematic indicators in stretched continental crusts (Ernst et al., 1995). In old magmatic provinces, dyke swarms can also provide structural and magmatic records for the roots of deeply eroded intrusive systems. This is particularly true for the Jurassic evolution of the Karoo–Antarctica LIP (KA-LIP) in relation to dispersal of the Gondwana supercontinent (Fig. 1a). Previous kinematic models of the KA-LIP were based on either petrological data (Brewer et al., 1992) or the spatial distribution of volcanic complexes (Burke and
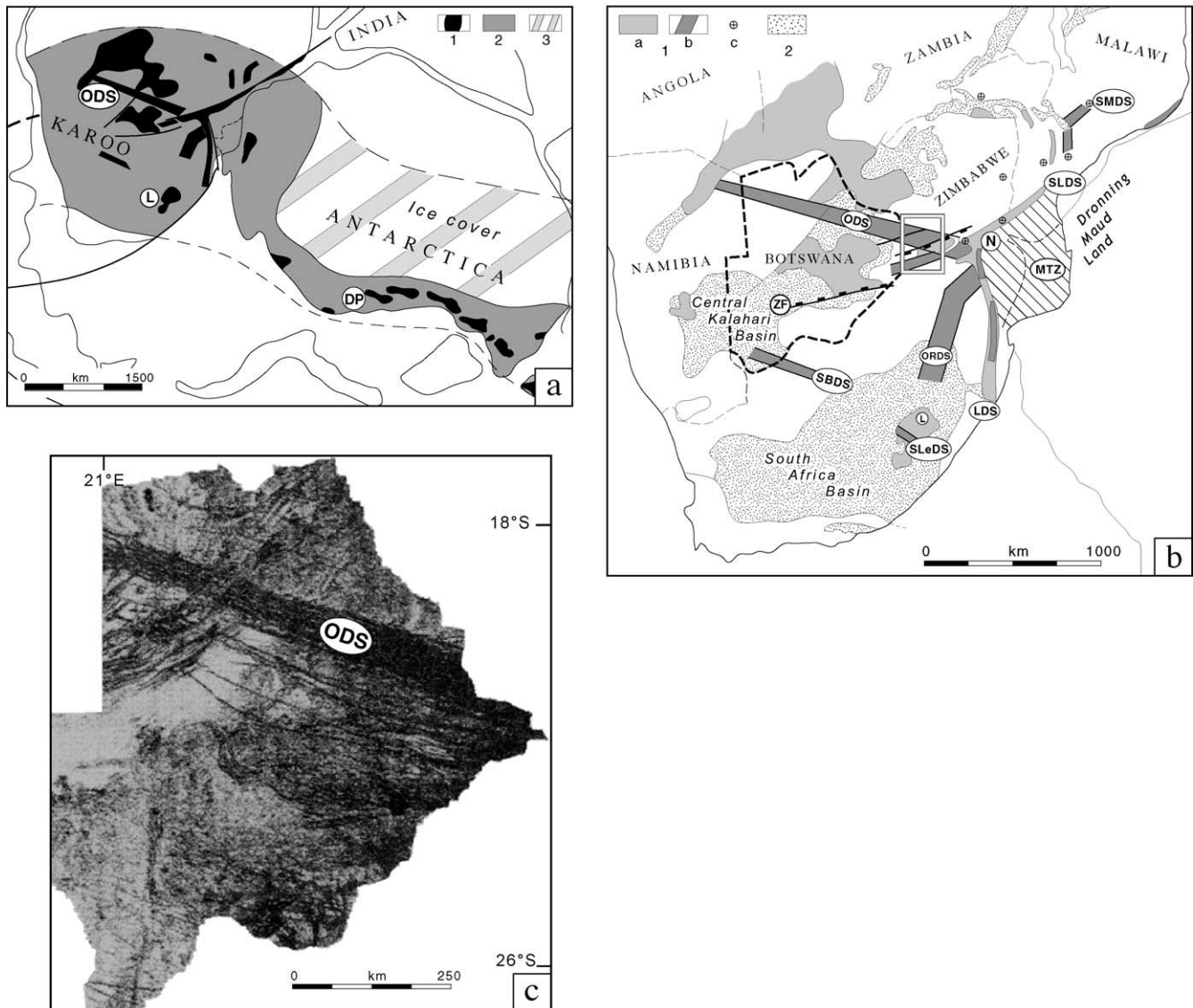
Fig. 1. (a) Distribution of continental flood basalt and related intrusive rocks of the Karoo–Ferrar/Antarctica LIP in a predrift Gondwana reconstruction: (1) exposed complexes; (2) extrapolated magmatic rocks; (3) inferred magmatic units beneath ice cover in western Antarctica. (b) Karoo tectono-magmatic framework of southern Africa. Inset shows the studied area in NE Botswana: (1) magmatic complexes with (1a) flood basalt, (1b) dykes and sills, and (1c) eruptive centres; (2) sedimentary basins. L, Lesotho; N, Nuanetsi; LDS, ODS, ORDS, SBDS, SLDS, SLeDS, SMDS, Lebombo, Okavango, Olifants River, South Botswana, Sabi-Limpopo, South Lesotho; South Malawi, dyke swarms, respectively. (c) Trace of the N110°/ODS on the low-resolution aeromagnetic map of NE Botswana (modified from Tshoso, 2003).

Dewey, 1972; White and McKenzie, 1989). Particularly, the large-scale radiating dyke systems centred in the Nuanetsi area (Fig. 1b) are regarded as convincing evidence for a mantle plume beneath the Karoo LIP (Campbell and Griffiths, 1990; Cox, 1992). However, detailed geochronological, petrological, and structural data on the Lebombo (NS), Olifants River (N20E°), Limpopo (N70E°) and Okavango (N110E°) dyke swarms forming the Nuanetsi triple junction-like pattern are lacking in their ability to firmly establish their synchronous and cogenetic emplacement as expected in the 'mantle plume' model.

This paper presents the first detailed quantitative structural study of two arms of the Nuanetsi triple

system, i.e. the N110°E-trending Okavango swarm (N110°/ODS) and part of the N70°E-trending Limpopo swarm (N70°/LDS), as exposed in NE Botswana. The main results are based on structural field measurements, integrated with ground and aeromagnetic data, from a 80-km-long section across the highest dyke density zone of the N110°/ODS. Compiling these data allows us to unravel the anatomy of a giant mafic dyke swarm and to investigate specific problems related to: (1) individual dyke geometry; (2) dyke opening directions; (3) dyke spatial distribution and frequency; and (4) geometrical and chronological relations of fracture networks and dyke swarms. Some new insights into the role of
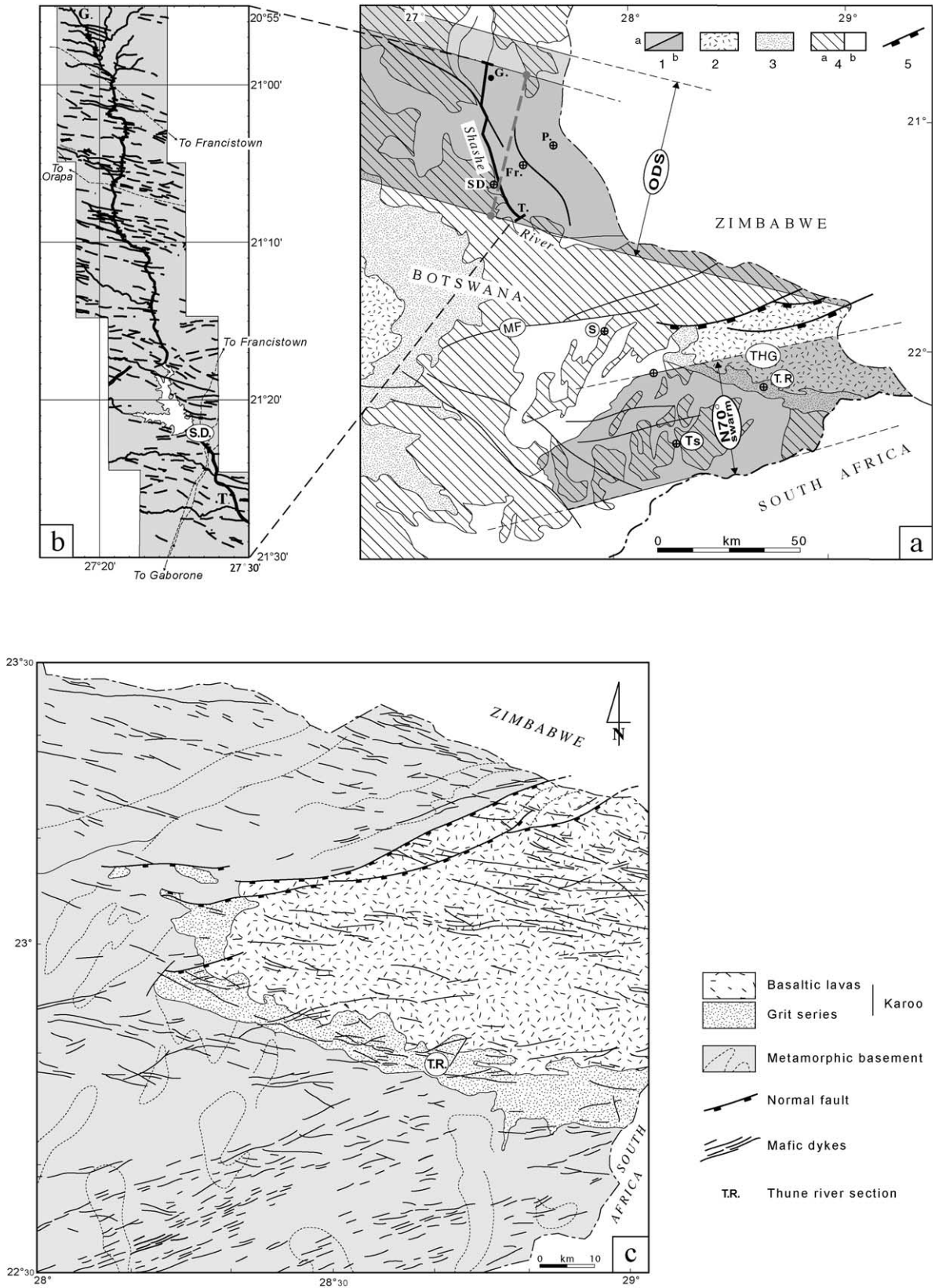
Fig. 2. The studied areas in the geological context of NE Botswana. (a) Simplified geological map. The Shashe reference section (and its projected trace in dashed line), the Tsetsebjwe (Ts) and Tuli (THG) sectors are shown: (1a) regional envelop of the highest density dyke zone in the N110 and N70° swarms; (1b) envelop of the swarm observed along the Shashe section; (2) flood basalt; (3) Karoo basins; (4) Precambrian basement with (4a) dominantly gneissic rocks, and

Precambrian structures on Karoo dyke emplacement in the LIP of NE Botswana are supplied by recent radiometric dating that demonstrate the polyphase origin of the N110°/ODS and N70°/LDS (Le Gall et al., 2002; Jourdan et al., 2004a).

2. Geological framework

From aeromagnetic records (Reeves, 2000), dykes in NE Botswana can be divided spatially into: (1) the ~100-km-wide N110°/ODS that strikes uniformly at N110°E over ~1500 km; and (2) the ~50-km-wide southwestern tip of the N70°/LDS to the SE (Fig. 1b and c). The two giant dyke swarms are partially exposed in the easternmost part of the country where they cut across basement crystalline rocks to the west (Shashe area), and Permo-Jurassic sedimentary and volcanic rocks in the Tuli half-graben further east (Fig. 2). Basement country rocks are mainly Neo-Archaean gneisses and granitoids of the Limpopo belt that were reactivated during the Palaeoproterozoic (McCourt and Armstrong, 1998). Their complex deformational history is shown by polyphase-folded ductile fabrics disrupted by variously trending shear zones and fracture networks. The overlying Permo-Jurassic cover consists of poorly strained terrigeneous sequences overlain by basaltic lava flows of the Stormberg series (Clark and Machacha, 1976).

In NE Botswana, N110 and N70°E dyke swarms and related lavas are exclusively composed of basalts, dolerites and minor gabbros, with geochemical compositions of quartz- or olivine-normative tholeiites (Jourdan et al., 2004a). Extensive Ar/Ar plagioclase dating of 40 dykes from the N110°/ODS cutting through Archaean rocks reveals that eight of them are Proterozoic in age, with no discriminative field characteristics (Le Gall et al., 2002; Jourdan et al., 2004a). The dated Karoo dykes (32 data) yield plateau ages between 179 ± 1.2 and 178.4 ± 1.1 My, with no across-strike age variation, hence indicating that they have intruded the crust over a short time span of 1–2 My, in agreement with previous radiometric age data for lavas in the northern Karoo LIP (Elburg and Goldberg, 2000; Jones et al., 2001). Similar ages are obtained from Karoo dykes in the N70°/LDS that also contain Proterozoic dykes (Jourdan et al., 2004a).

3. Data acquisition

The present work focuses on the broad structure of the

two giant mafic dyke swarms, as well as on the shape and internal structure of individual dykes. Exposures are usually limited in extent, hampering investigation of the 3D geometry and along-strike characteristics of dykes. However, exceptionally good exposures at a few localities (Shashe Dam, Thune River) allow detailed mapping of the dyke system. The cornerstone of our investigation is the ~80-km-long Shashe river bed that cuts at a high angle through the densest zone of the N110°/ODS within basement country rocks (Fig. 2b). Among 171 dykes identified along the exposed portions (~58%) of the Shashe profile (Fig. 3b), 153 dykes have been measured in terms of strike, dip, and width (Table 1). The accuracy of field data in this paper is 0.5 m for the dyke width and a few degrees for their strike and dip. The greater number of dykes (423) detected along this profile using ground magnetics (Tshoso, 2003) allows us to estimate the dyke-induced dilatation on the 52-km-long section projected perpendicular to the trend of the swarm. This value is then extrapolated to the total width (60 km) of the highest dyke density zone drawn from regional aeromagnetic maps (Fig. 2a).

Because of the polyphase nature of the N110°/ODS, which is now known to involve both Proterozoic and Jurassic dykes, the statistical analysis of field and aeromagnetic data must be carried out with caution to ensure focus on the Karoo dyke component. For that reason, the Shashe section has been subdivided into three distinct segments with respect to the spatial distribution of Proterozoic and Karoo dykes (Fig. 3c). The 22-km-long central segment (II) comprises 8 (30%) Proterozoic dykes and 18 (70%) Karoo dykes, whereas the two external segments (I and III) are assumed to be exclusively composed of Karoo dykes. Applying the corresponding ratios of Karoo vs. total dykes for segments I, II and III (i.e. 100, 70 and 100%) to the entire dyke population (423 data) suggests that the Okavango giant dyke swarm may comprise around 370 Karoo dykes (ca. 87%) along the Shashe transect. A nearly similar dyke ratio is deduced from the map distribution of dykes on either side of the northern border of the Tuli half-graben to the east (Fig. 2c). Herein, the term N110°/ODS only refers to the Karoo part of the Okavango polyphase dyke complex. A much higher (not precisely defined) ratio of Proterozoic vs. Karoo dykes is deduced for the composite N70°/LDS from the contrasted density of mapped dykes on both sides of the Tuli half-graben (Fig. 2c).

From field investigations in the Tsetsebjwe (N70°/LDS across basement) and Thune (N110°/ODS across Permo-Jurassic cover) areas (Fig. 2a), assessments about the role of country rock lithology on the across- and along-strike variations in structural styles of the dykes are attempted.

(4b) granites; (5) extensional faults. Fr, Francistown quarry; G, Gulubane; ODS, Okavango dyke swarm; P, Phoenix quarry; SD, Shashe Dam; T, Tonotha; TR, Thune river section; TS, Tsetsebjwe section. (b) Map-view of the Shashe section. The dyke pattern (from Aldiss, 1986) is too intense to be shown in its entirety. (c) Mapped distribution of N110°/ODS and N70°/LDS dykes at the periphery of the Tuli half-graben (from 1:125,000 maps (Geological Survey of Botswana) of Magogaphate (Bennett, 1969), Semolale (Aldiss, 1982), Tsetsebjwe (Aldiss, 1981), and Baines Drift (Clark and Machacha, 1976).

Table 1
Dyke dataset acquired in the three areas under study

		Geological Survey of Botswana	This work							
			Field data					Ground Magnetic data		
			Identified	Measured		Dated		Inferred age		
				Width	Complete	Karoo	Basement	Karoo	Basement	
N110°E swarm	Shashe section	46	171	171	81	32	8	366	57	
	Thune section	×	15	15	15	×	0	No	No	
N70°E swarm	Tsetsebjwe	×	14	14	0	1	1	No	No	

The limited number of dykes measured in these two areas cannot be statistically representative of the regional patterns, but the quantitative parameters (width, total dilatation) on these dykes may be compared with those of the N110°E Karoo dykes along the Shashe section.

4. Geometry of dykes

Most of the geometrical data constraining Karoo dyke emplacement mechanisms are obtained from N110°/ODS dykes exposed in horizontal surfaces along the Shashe section. Emphasis is placed on the width parameter. Additional 2D structural information about strike and length dykes are supplied by published 1:125,000 geological maps (Geological Survey of Botswana) covering the densest zones of the N110°/ODS and N70°/LDS (Fig. 4).

4.1. Strike

The dyke networks drawn on the Shashe and Tsetsebjwe maps from aerial photographs (Aldiss, 1981, 1986) do not discriminate the two chronologically unrelated dyke populations (Proterozoic and Middle Jurassic in age) that
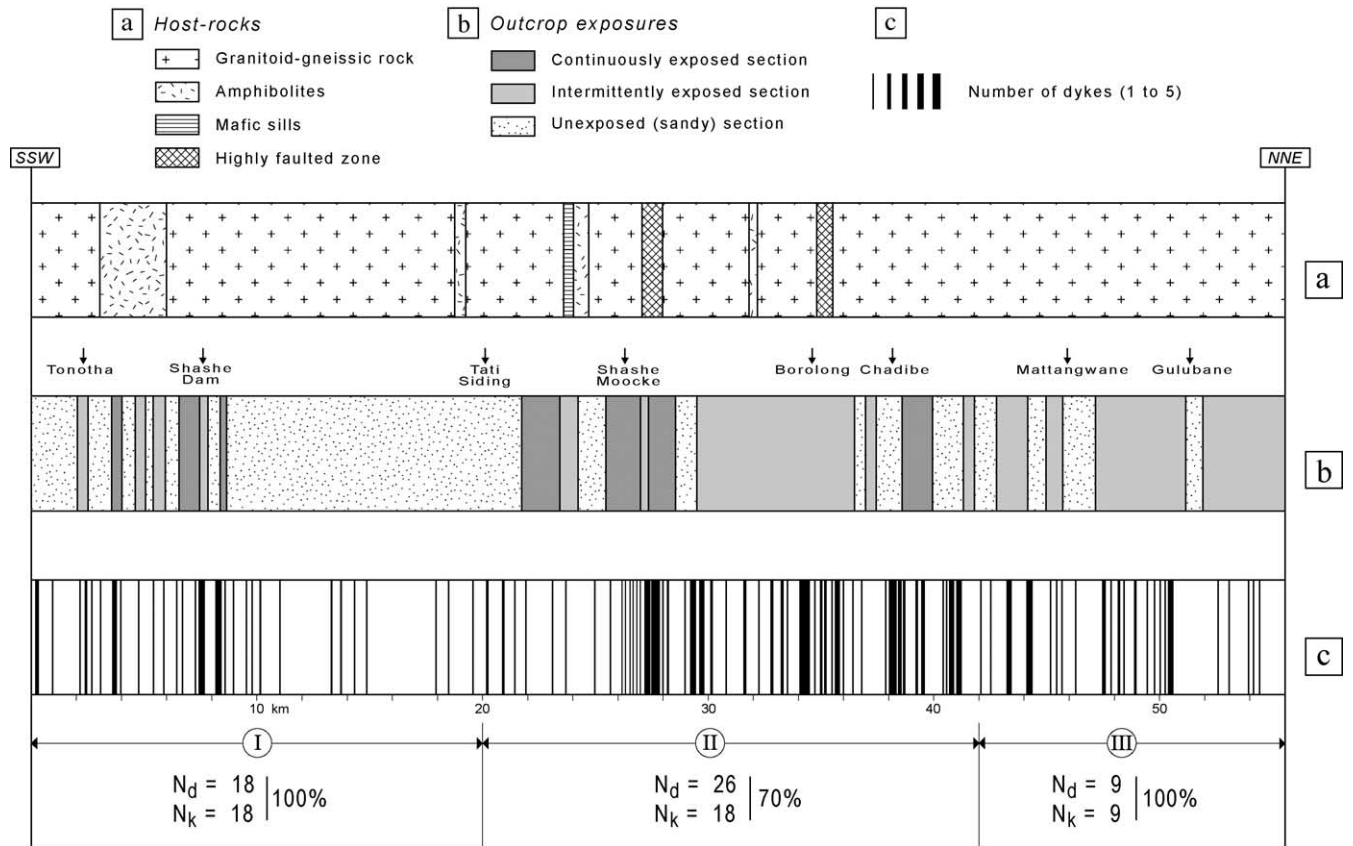

Fig. 3. The Shashe reference section projected perpendicular to the N110°E trend of the ODS. (a) Host-rocks; (b) conditions of exposure; (c) frequency distribution of dykes in the field. I, II, and III are segments discussed in the text. N_k is the Karoo dyke population within the total number of dated dykes (N_d); the corresponding percentage of Karoo dykes is indicated.

have been since identified (Le Gall et al., 2002). Because of the estimated high percentage (87%) of Karoo dykes in the N110°/ODS, these limitations are assumed not to bias our statistical analysis.

The cartographic arrangement of 628 dykes from the N110°/ODS and 201 dykes from the N70°/LDS (Shashe and Tsetsebjwe sheets in Fig. 4a1 and b1) indicates a preferred dyke orientation within each swarm. About 70% of dykes in the ODS are within 10° of parallelism with the N110° trend of the swarm envelope (Fig. 4a2), but with a marked asymmetry (greater frequency of N100°E dykes), which is not easily interpreted because of the uncertainties about cross-cutting relationships and origins (inherited or newly formed) of the different dyke trends. A stronger parallelism for the dykes in the N70°/LDS is shown by 95% of dykes oriented between N60–N80°E (Fig. 4b2). Rapid changes of dyke azimuth are only reported at a smaller scale from field observations about N110°/ODS dykes in both basement and Permo-Jurassic terrains (see Section 4.6).

4.2. Length

Karoo dyke length ranges from 1 to 18 km for N110°/ODS and 1 to 14 km for N70°/LDS (Fig. 4a1 and b1), but dykes generally display a relatively short strike length of 3.0 km on an average for both swarms (Fig. 4c).

4.3. Dip

The dip of 82 dykes along the Shashe section indicates that ∼91% of dykes are vertical, and the remaining 9% are within 30° of the vertical (Fig. 5a). Most inclined dykes show striated walls that typify reverse fault surfaces trending at ca. N110°E. Since syn- to post-Karoo compression is not yet documented in Botswana, the reverse fault planes likely originated as Archaean/Proterozoic structures that were later locally injected by Karoo magma. In contrast, Karoo dyke attitude in the Permo-Jurassic series of the Thune river section differs significantly since dykes dip consistently 70–80°S, throughout shallowly dipping (∼20°) strata (Fig. 5c and d). The entire dyke/host-rock system is dissected by a dense array of dyke-parallel normal faults that preferentially reactivate dyke margins with a dominantly dip-slip component (Fig. 5b and e). The dipping attitude of the overall dyke/host-rock system is assigned to extensional fault-block rotation coeval with dyke intrusion in Middle Jurassic time on the southern margin of the Tuli half-graben.

4.4. Width

The width of N110°/ODS dykes is constrained using: (1) field measurements that provide an incomplete, but accurate dataset; and (2) ground magnetic records that supply a complete dataset, but with no certainties on the age of the mapped dykes. Field measurements were principally

acquired on dykes intruding the Archaean basement along the Shashe transect (Fig. 2b). For each dyke, the width is measured normal to its main strike. Whether eroded or not exposed, the contact between the dyke and its host-rock can usually be located within 0.5 m, hence defining the resolution limit of field measurements.

The dyke width estimates from ground magnetic records are deduced from the shape of the corresponding magnetic anomaly (Tshoso, 2003). Dyke boundaries are located by the inflection points of the deskewed magnetic anomaly signal with a lateral resolution of 1–6 m that depends on the altitude of the measurements above the magnetized dykes (expected to range between 2 and 12 m). With a sampling interval of the ground magnetic signal of 5–10 m, it is likely that a number of dykes narrower than 5 m may not be detected. For similar reasons, dyke widths estimated from the ground magnetic signal may be in error by several metres. Despite these limitations and given the great number of both magnetic ($N = 423$) and field data ($N = 171$), statistical analyses of dyke widths are attempted, first in terms of class distribution for both the total (Karoo and Proterozoic, K–P) and Karoo (K) dyke populations. To avoid additional errors, the Karoo dyke component of the composite segment II (see Fig. 3c) is not included in the K population, which is thus $N = 236$ (ground magnetic data) and $N = 83$ (field data).

Width-scaling properties are also investigated from conventional cumulative frequencies in order to test the 'self-similar' behaviour of the width population, as well as the power-scaling law distribution classically observed for 2D structures (Scholz and Cowie, 1990). Histograms of K–P and K subsets show dyke widths ranging from 0.2 to 69 m (Fig. 6a–d). Magnetic data (K–P and K populations) display unimodal distributions, marked by a progressive decreasing frequency of dykes from a mode value of 11 m to a maximum value of 69 m (Fig. 6a and b). The drastic decreasing number of values from $N = 110$ (class 10–15 m) to $N = <30$ in the lowest class (0–5 m) is also noticeable, and further discussed below. The calculated arithmetic mean widths are 17.5 (K–P) and 17.1 m (K), respectively. Quite similar mean dyke widths are obtained from field measurements of K–P (16.1 m) and K (15.9 m) dyke networks (Fig. 6c and d). The small frequency of narrow dykes (<5 m) also observed on K–P and K field data plots, values that are much greater than the field resolution (0.5 ≪ 5 m), is assumed not to be an artefact due to a sampling effect. Consequently, and despite the lack of resolution of the magnetic records for dykes <5 m thick, the low frequency of narrow dykes depicted from magnetic data may indeed be a real feature.

The scaling properties of width populations have been investigated further using conventional cumulative frequency vs. width distributions (Fig. 6e–h). Data plotted in log–log space permit identification of eventual fit to power-law distribution defined by:
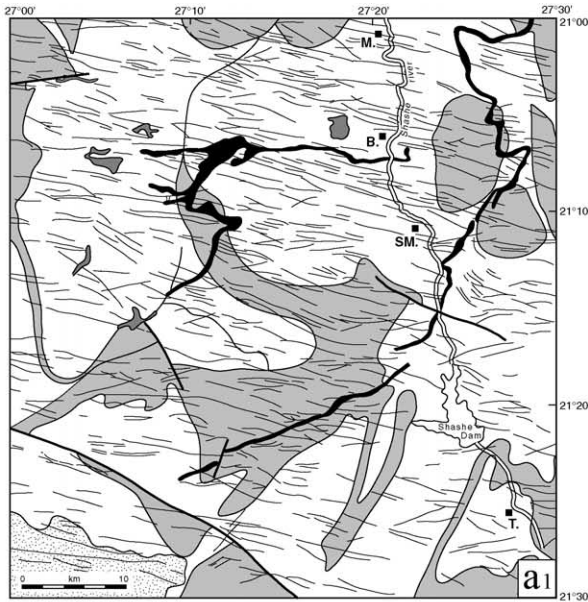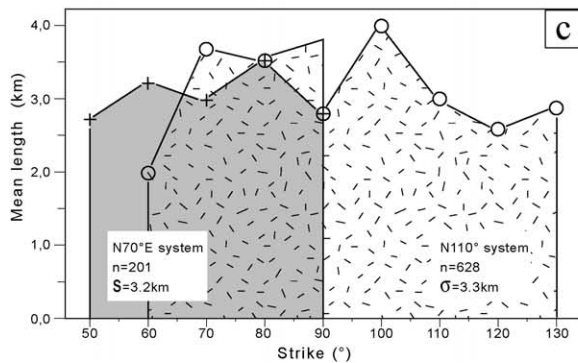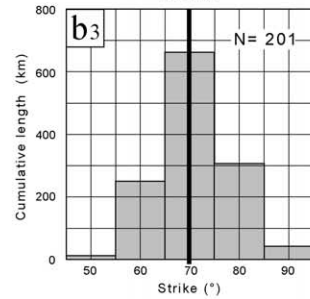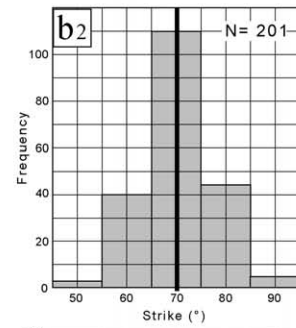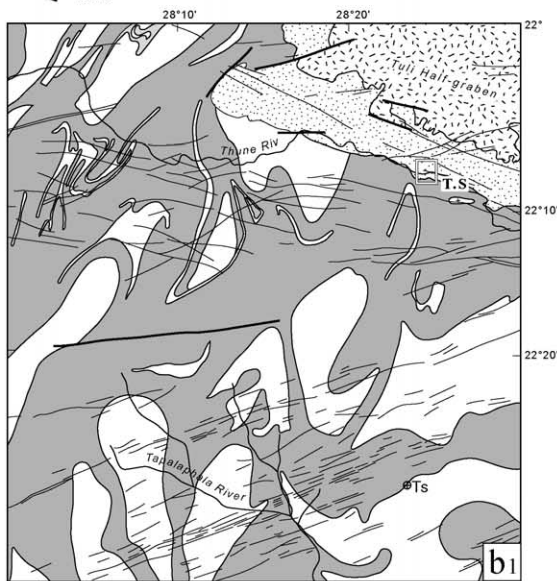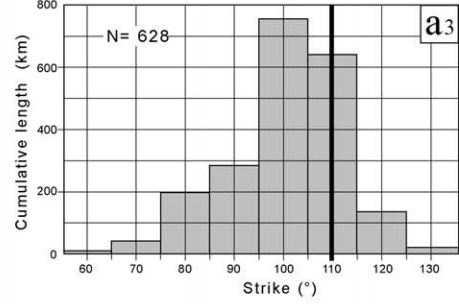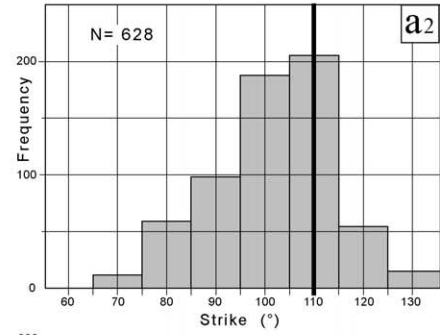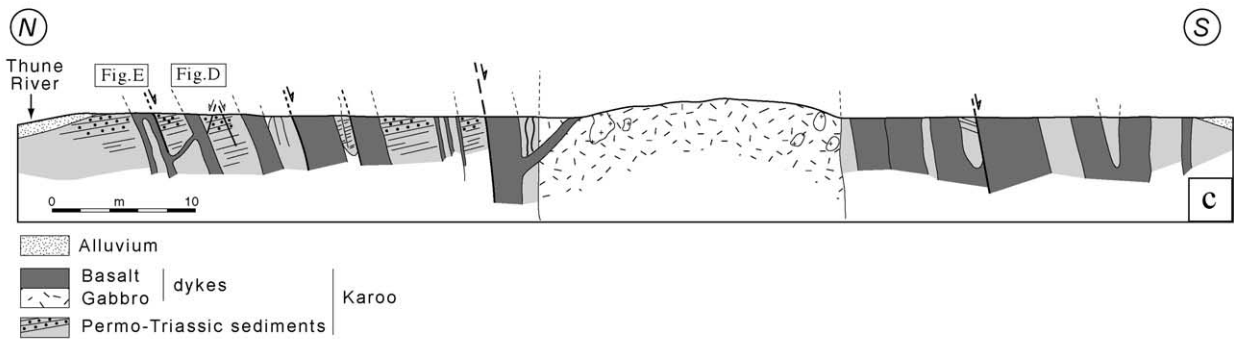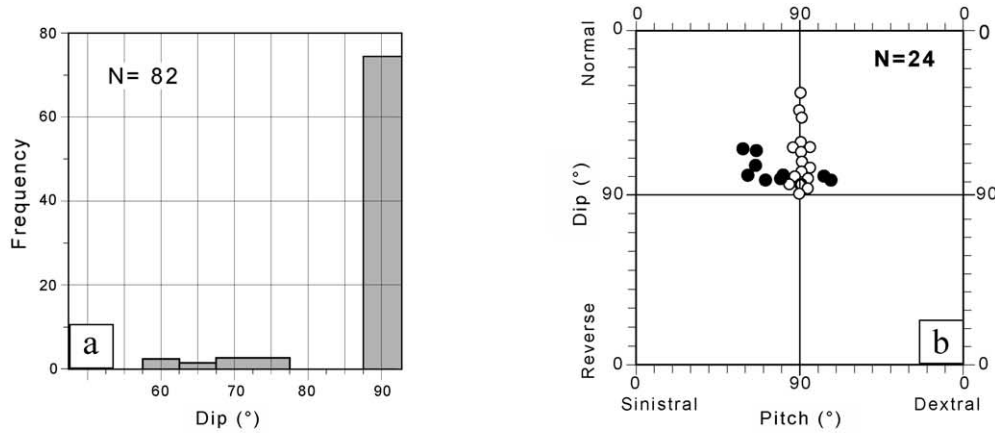
Fig. 5. Dip attitude of dykes and faults in the N110°/ODS. (a) Dip distribution of 82 dykes in the Shashe section. (b) Diagram of fault dip vs. striation pitch measured in the Thune section (location in Fig. 2a and c). (c) The Thune river cross-section along the southern margin of the Tuli half-graben. (d) Inclined attitude of a 60-cm-wide Karoo dyke intruding shallowly dipping grit strata (location in Fig. 5c). (e) Karoo dyke wall reactivated as a dip-slip normal fault (location in Fig. 5c). Near-vertical slickensides plunge 80° to the S. The picture is oblique to the fault plane.

$$N(W) = \alpha W^{-C} \qquad (1)$$

where N is the number of dykes with width greater than or equal to W, α is a constant, and C is the power-law exponent

that also gives the fractal dimension of the population under study (Childs et al., 1990). Examination of dyke widths (K–P and K subsets) from magnetic and field datasets suggests that the N110°/ODS does not ascribe to a single power-law

Fig. 4. Strike distribution of Karoo dykes in (a) the N110°/ODS and (b) the N70°/LDS. (a1) Cartographic arrangement of N110°/ODS dykes in the Shashe 1: 125,000 geological sheet (simplified from Aldiss, 1986). (a2) Frequency histogram of strike data. (a3) Cumulative length vs. azimuth diagram. (b1) Spatial distribution of N70°/LDS dykes in the Tsetsebjwe 1:125,000 geological sheet (simplified from Aldiss, 1981). (b2) Dyke length/orientation diagram. (b3) Cumulative length vs. azimuth diagram. (c) Mean length/orientation diagram for dyke populations in the N70 and N110°E swarms.

Fig. 6. Width-scaling properties for dykes in the N110°/ODS. (a)–(d). Frequency of dyke widths from aeromagnetic ((a) and (b)) and field ((c) and (d)) data. *N*, number of data; μ, mean; σ, standard deviation; *m*, mode. (e)–(h) Log–log cumulative frequency–width plots for the aeromagnetic ((e) and (f)) and field ((g) and (h)) dyke populations, and fit with statistic power-law models. See text for explanations.
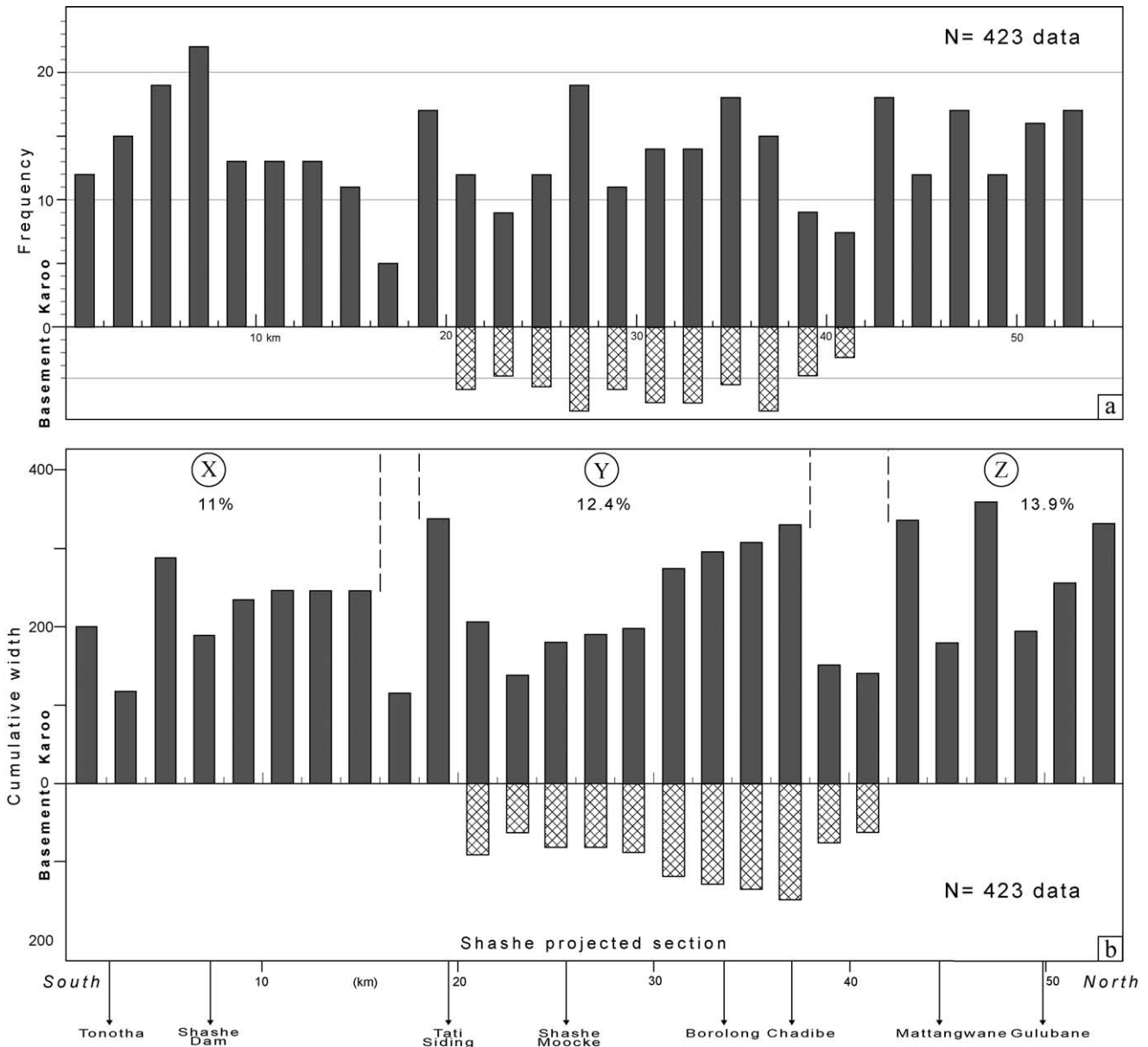
Fig. 7. Frequency and cumulative width of dykes in the projected Shashe section. (a) Distribution of Karoo (upper part) and basement (lower part) dykes per 2 km interval, from field observations. (b) Cumulative width of dykes (in meters) as deduced from ground magnetic anomaly mapping. X, Y, and Z (and the corresponding percentage of dyke-induced dilatation) are segments discussed in the text.

model (Fig. 6e–h). The population distributions on log–log plots do not exhibit self-similar properties and provide non-linear curves that are not assigned to sampling issues (see above) such as truncation at small width (resolution effects) or censoring at large widths (dyke widths are much lower than the total width of the dyke swarm). Each curve is segmented into two or three straight line portions (P in Fig. 6e and h) corresponding to potential power-law functions. It has been shown elsewhere that even though a total 2D population does not show a single power-law size distribution, it may contain sub-populations that do (Fossen and Rornes, 1996). In the case of the N110°/ODS, the narrower dykes tend to form sub-populations (P1),

occurring for width <11 m, that closely follow power-law width distributions with a low exponent $C \sim 0.4$. Second portions (P2) are observed for dyke width values ranging between 16 and 28 m and fitting with power-law dimensions of C between 1.57 and 1.82. The break in slopes between P1 and P2 occurs on all diagrams for a width value of ~ 11 m (Fig. 6e–h), higher than the field resolution, corresponding to the mode statistic parameter. A simple explanation for this break in slopes still remains to be found. The last portions (P3), comprising the widest dykes (28–69 m), could be defined by power-law exponent $C \sim 3$ (Fig. 6e and f). Indeed, P1 and P3 are controlled, respectively, by excessively low or high exponents that are significantly
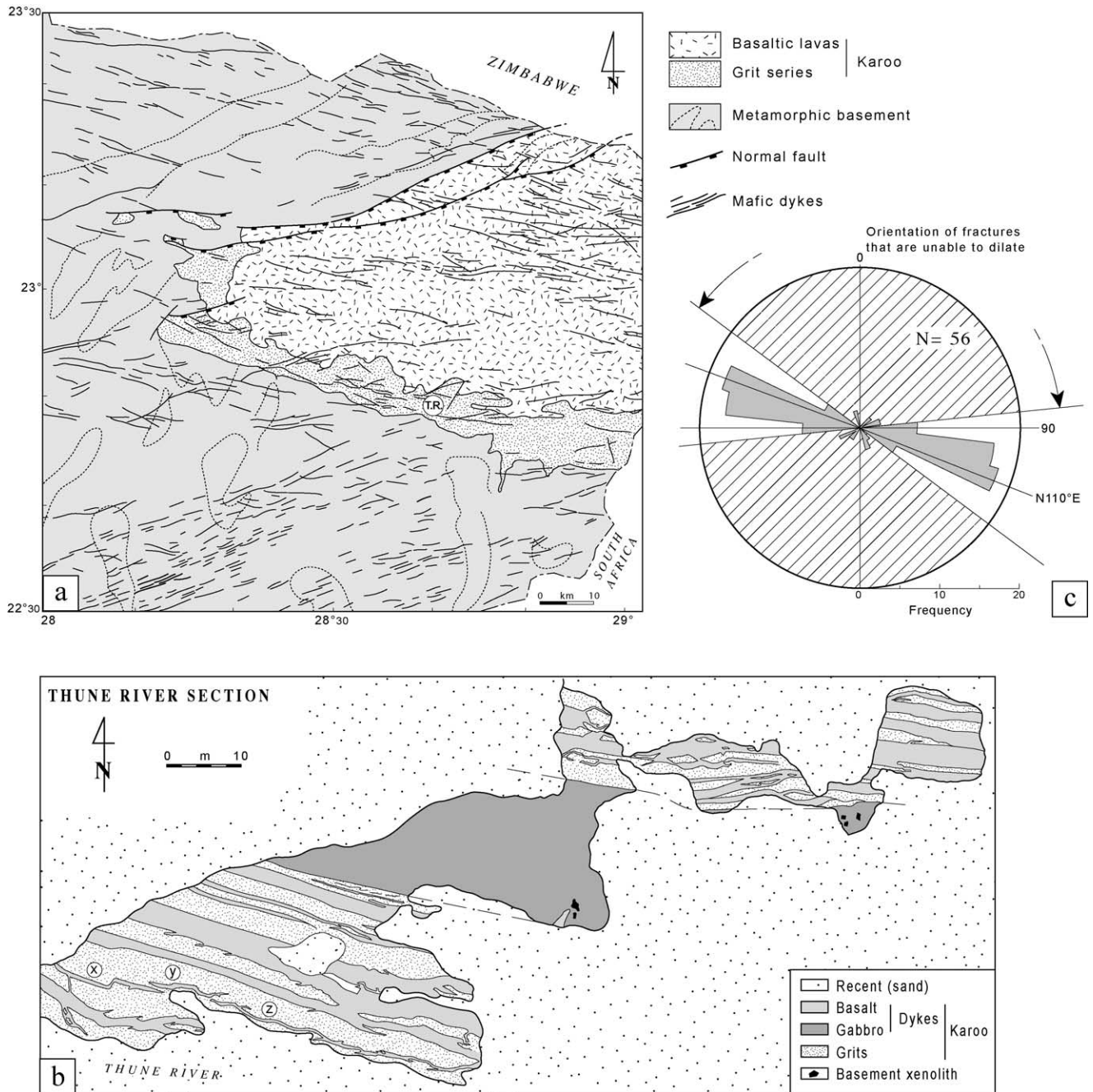
Fig. 8. 2D geometry (horizontal-view) of Karoo dykes intruding Permo-Jurassic sedimentary rocks in the southern margin of the Tuli half-graben. (a) Location of the Thune river section (TR) on a simplified geological map. (b) Cartographic distribution and shape of a braided dyke system. (c) Rose-diagram showing the restricted range of dyke/fracture orientations.

different to the usual 1–2 range (e.g. P2) typically assumed for 2D structures (Cladouhos and Marrett, 1996). It is thus believed that the lower dyke width population (<11 m) is under-represented on histograms and cumulative log–log frequency diagrams when plotting the magnetic and field dataset of K–P and K populations.

When comparing field dyke widths from the Shashe (171 data), Tuli (13 data), and Tsetsebjwe (13 data) areas, there is a clear increase in Karoo dyke width from 1.3 (N110°E

dykes intruding sedimentary rocks, Tuli half-graben) to 18 (N110°E dykes cutting across Archaean basement, Shashe area), up to 27 m (N70°E dykes intruding crystalline basement, Tsetsebjwe area).

4.5. Dyke distribution and cumulative dilatation

The 2D distribution of Karoo dykes in the N110°/ODS is also constrained using both field and ground magnetic data

along the Shashe section. On well-exposed areas, field observations indicate that the N110°/ODS consists of individual dykes separated by large areas containing no intervening mafic dykelets (in agreement with the statistical results above). The frequency of Karoo dykes deduced from ground magnetic records has been calculated for 2 km intervals, one each segment (I, II and III) by applying the corresponding Jurassic/total dyke ratios of 100 (I and III) and 70% (II). The histograms in Fig. 7 show three high-density dyke zones, each ∼15 km wide, labelled X (108 dykes), Y (118 dykes) and Z (92 dykes), with dyke frequencies ranging from 10 to 22 dykes/2 km^{-1}, and separated by two narrow low-density dyke zones.

The frequency and spacing of Karoo dykes, expressed as the volume percentage of rocks composed of dykes, is used to infer the amount of dilatation along the Shashe section (Fig. 7b). Total dilatation (*D*) is obtained by projecting the dykes onto a line that is drawn perpendicular to the envelope of the swarm and dividing the cumulative dyke width by the length of the line (Gudmundsson, 1990b):

$$D = \frac{\sum w \times 100}{L} \qquad (2)$$

where *w* is the cumulative width of dykes, and *L* the length of the projected section.

The cumulative dyke width ($\sum w$) deduced from ground magnetic data (Tshoso, 2003) is 6315 m. In terms of finite strain, it corresponds to a dyke-induced dilatation of 12.2% in the 52-km-long projected section. Extrapolating this value to the total width (60 km) of the highest dyke density zone suggests, at first approximation, a dyke-driven extension of ∼7300 m in the N110°/ODS. Fig. 7b also illustrates the inhomogeneous distribution of dilatation across the N110°/ODS. Transects with high dilatation of nearly 20 (2 km long Tati Siding and Mattangwane sections) and 16% (4 km long Borolong section) alternate with lower dilatation transects of <2% (2 km long Tonotha and S Tati Siding sections). The inhomogeneous distribution of dyke-induced dilatation coincides with dyke frequency along the projected section (Fig. 7a and b).

4.6. Shape of dykes

Karoo dykes are better exposed throughout the N110°/ODS cutting across basement (Shashe river) and Permo-Jurassic (Tuli half-graben) country rocks. Generally, dyke margins are almost invariably sharp, and thickness rarely changes along-strike. Marked contrasts of the 2D geometry of dykes are documented as a function of the sedimentary or crystalline nature of the host-rocks. When the 3D geometry of dykes is observed (Shashe Dam and Thune section), information is also supplied on their relationships to basement and Karoo structures, and on kinematics of dyke emplacement.

4.6.1. Permo-Jurassic host-rocks

Karoo dykes exposed along the southern flexural margin of the Tuli half-graben (Thune section) (Fig. 2c) cut through basal and fine-grained terrigeneous sequences of the Permo-Jurassic succession. In a 150×200 m^2 area along the Thune river, grit strata plunging shallowly to the north (see Fig. 5c), are cut by 12 thin (1–2 m thick on average), connected dykes that are symmetrically distributed on both sides of a 20-m-wide gabbroic body striking N105°E (Fig. 8b). Dykes form a braided system resulting locally in elongated country rock bodies totally engulfed by mafic dykes. Of the 56 dyke azimuths measured in this area (with several data on each individual dyke), 80% lie between N90 and 120E° (Fig. 8c). This low range of orientations is due to either the rectilinear trace of the wider (∼1–2 m) dykes or the smooth and sinusoidal trajectory of <50-cm-wide and unconnected dykes (X, Y and Z in Fig. 8b) that show no pronounced offsets.

4.6.2. Basement crystalline host-rocks

A wider azimuth range typifies dykes of the N110°/ODS cutting through Archaean basement in the Shashe area. The distribution of six closely spaced Karoo dykes and dykelets in the Phoenix quarry, 50 km east of the Shashe section (Fig. 2a), is shown in Fig. 9a. Strike changes of ca. 50° originate from predominantly right lateral steps related to a set of fractures striking in the azimuth N75–125°E, although 70% of dykes trend N90–110°E (Fig. 9b).
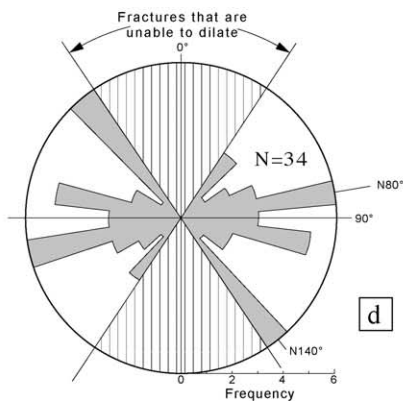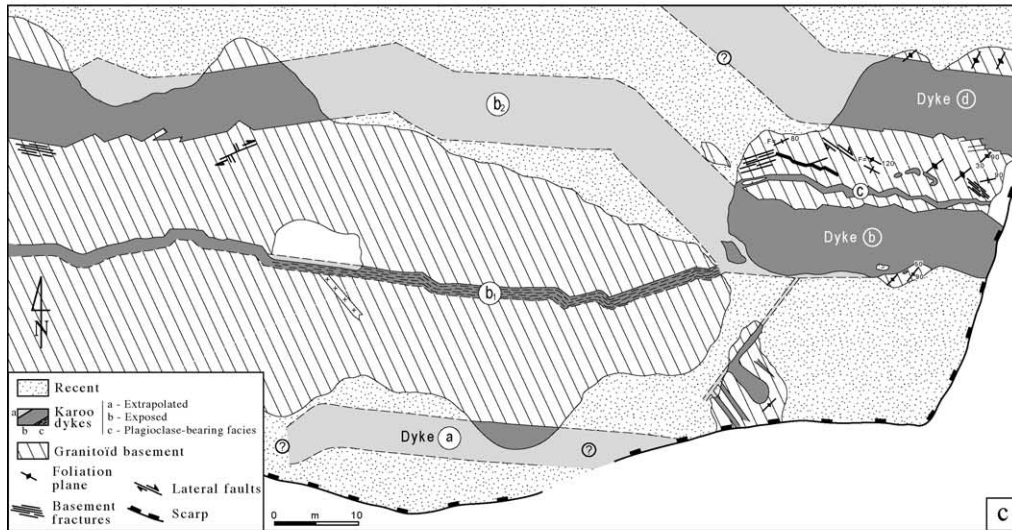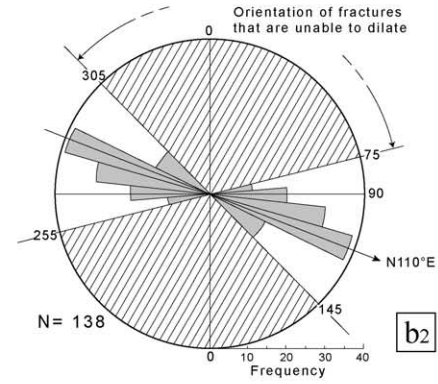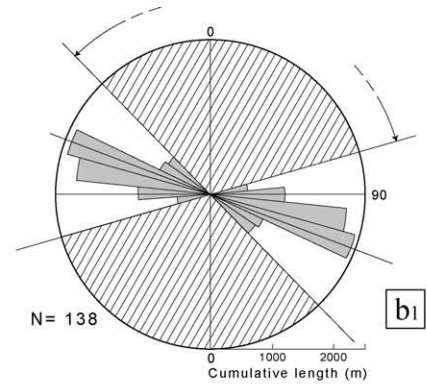
In the southern part of the Shashe section (Shashe Dam in Fig. 2a and b), nearly unbroken exposures over ∼200× 400 m^2 allow detailed mapping of a complex linked dyke array comprising three main dykes (named a, b and d), ∼20 m wide each, and striking at N80–110°E (Fig. 9c). Dyke 'b' splits westwards, via oblique diverging dyke segments, into two dykes (b1 and b2) with highly segmented geometries. Right stepping offsets of dyke margins are dominant. Segmented dykes are formed of 5–60-m-long segments showing a wide range of strikes between N65 and 120°E, linked by shorter (1–30 m long) segments with a narrow spectrum of orientations at N120–140°E. The azimuth dispersal of the zigzag dyke pattern shows two peaks at N80 and N140°E (Fig. 9d). Walls of the dyke segments are generally simple planar contacts, but they are locally disturbed by asymmetric and low-angle bayonet-like apophyses that are well displayed in dyke 'c', for example (Figs. 9c and 10a).

5. Conditions of dyke emplacement

On the basis of the above-mentioned geometrical parameters, a number of assumptions about the mechanisms of Karoo dyke injection are attempted below.

5.1. Dyke emplacement stages

Most individual dykes show a well-developed centi-metre-wide aphyric chilled margin and enclose very few

Phoenix quarry

Trace of dykes

0   m   200

a

N= 138

Cumulative length (m)

b1

Orientation of fractures that are unable to dilate

N= 138

Frequency

N110°E

b2

Recent

Karoo dykes
a - Extrapolated
b - Exposed
c - Plagioclase-bearing facies

Granitoïd basement

Foliation plane

Basement fractures

Lateral faults

Scarp

0   m   10

c

Dyke d

Dyke b

Dyke a

Fractures that are unable to dilate

N=34

N80°

90°

N140°

Frequency

d

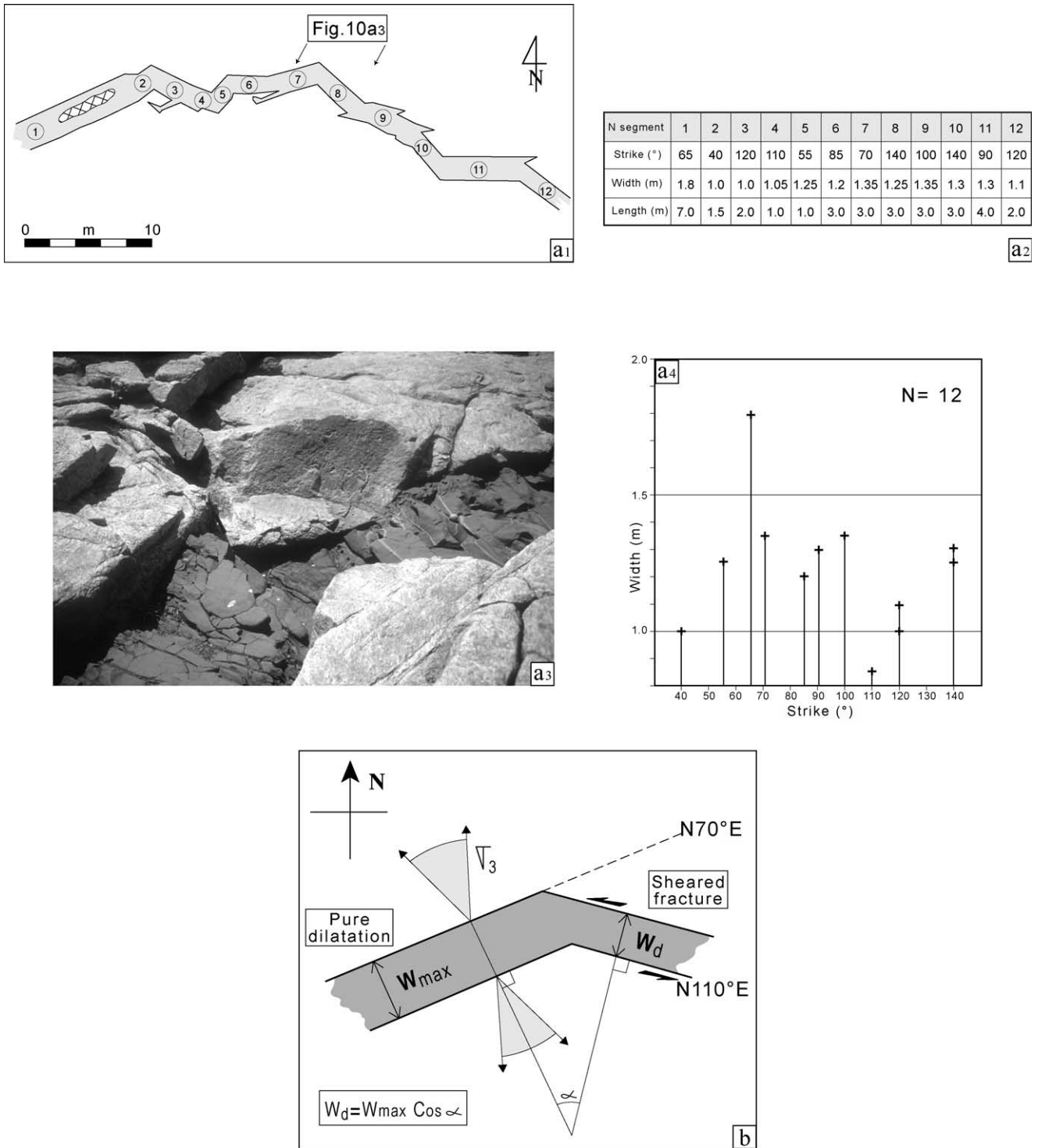| N segment	1	2	3	4	5	6	7	8	9	10	11	12
Strike (°)	65	40	120	110	55	85	70	140	100	140	90	120
Width (m)	1.8	1.0	1.0	1.05	1.25	1.2	1.35	1.25	1.35	1.3	1.3	1.1
Length (m)	7.0	1.5	2.0	1.0	1.0	3.0	3.0	3.0	3.0	3.0	4.0	2.0

Fig. 10. Direction of dyke dilatation in the N110°/ODS (Shashe section). (a) Geometrical data from the segmented dyke 'c' of Fig. 9c. (a1) Mapped geometry. (a2) Compiled strike, width and length data. (a3) Field-view of the zig-zag pattern between dyke segments 7 and 8. (a4) Width/strike diagram of 12 dyke segments drawn in (a1). (b) Sketch map-view showing variations of dyke thickness as a function of the angle (α) between the dyke azimuth and the direction of regional extension.

Fig. 9. Form of N110°/ODS dykes cutting across Precambrian metamorphic rocks in the Shashe area. Map-view (a) and strike attitude (b) of Karoo dykes in the Phoenix quarry (see location in Fig. 2a). (b1) and (b2) Frequency and cumulative length distributions of dykes vs. azimuth. (c) Detailed structural map of the Shashe Dam area (see location in Fig. 2a) showing the segmented geometry of most dykes. (d) Rose-diagram of dyke segment orientations.
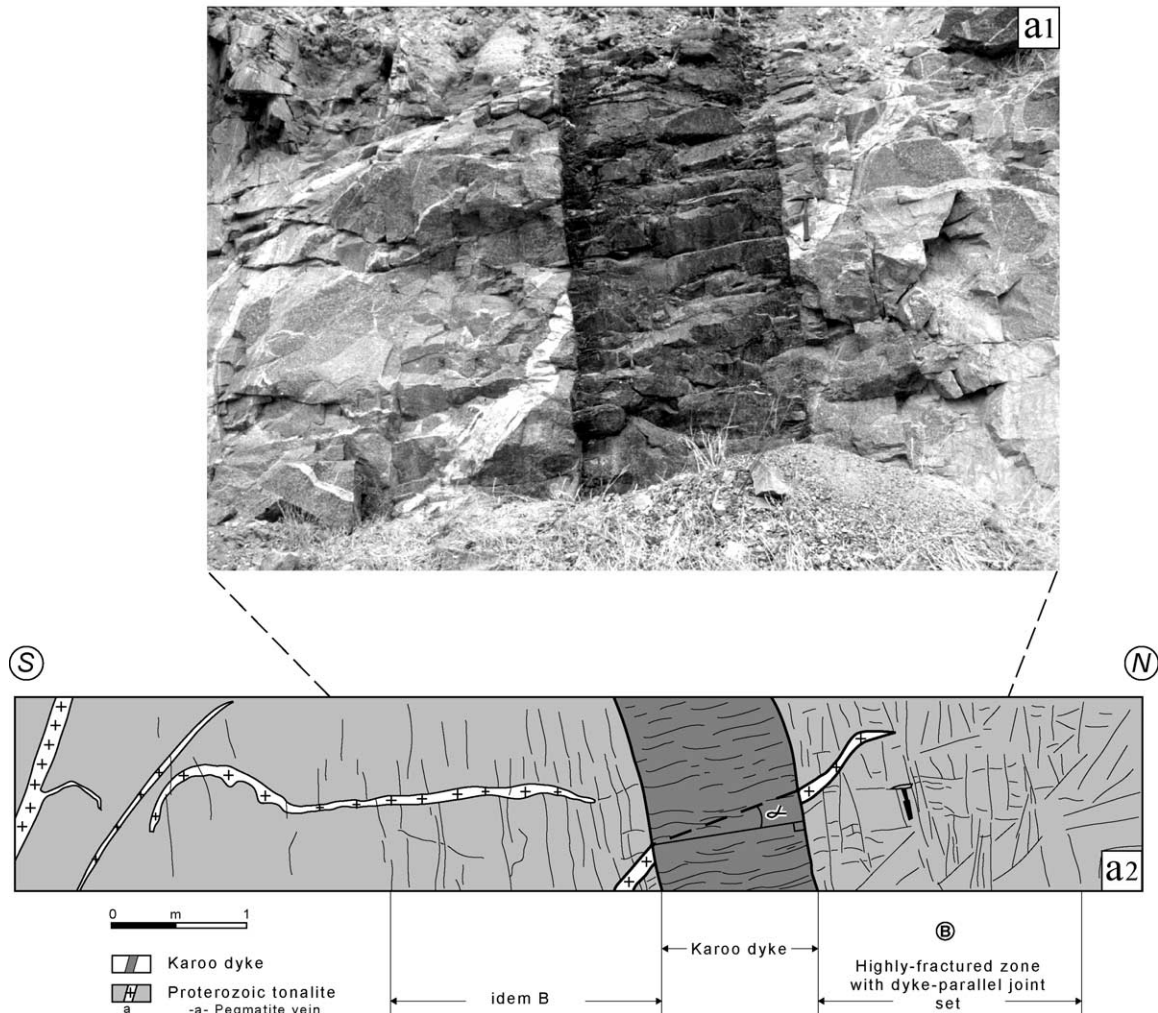
Fig. 11. Field evidence for dyke-induced brittle deformation in Precambrian tonalitic basement host-rocks in the Francistown quarry, Shashe area (location in Fig. 2a).

crustal xenoliths. Furthermore, there are neither significant brecciated wall rocks nor distortion in the intruded rocks, suggesting that emplacement of dykes was not forceful. This is in agreement with the lack of any internal strain. Dyke geometries generally observed in the N110°/ODS indicate that dyke fissure dilatation is a single event. There are only a few cases of multiple-stage dykes recording a repetition of the fracture–dilatation–magma injection sequence.

5.2. Direction of fracture opening and palaeostress field

Pre-existing discontinuities may play a strong tectonic control on dyke geometry when magma is emplaced throughout highly strained terrains. In these conditions, dykes usually follow inherited fractures that do not necessarily lie perpendicular to the applied least compressional stress, and their orientation cannot be used to infer paleostress direction (Delaney et al., 1986). Alternative criteria, such as dyke width changes, may supply

information about the extension direction that prevailed during dyke emplacement (Baer et al., 1994). One first notices that Karoo segmented dykes in the N110°/ODS show no systematic width changes with a change in strike when studied at a local scale (Shashe Dam site, for example) (Fig. 10a1 and a2). Significant dyke width variations are only evidenced at a regional scale when comparing the average dyke width in the N70°/LDS (27 m) and the N110°/ODS (~17 m). If we assume that the two swarms were emplaced: (1) synchronously (Jourdan et al., 2004b); (2) under homogeneous extension; and (3) with a similar magma viscosity—known to partly control dyke width (Wada, 1994) and deduced here from close chemical compositions and phenocryst contents (Jourdan et al., 2004a); the estimated thickness changes are likely to be a function of dyke orientation with respect to the applied stress field. Baer and Beyth (1990) proposed that the thickness of a given dyke segment (d) forming an angle α with the optimally oriented segment of maximal thickness (W_{max}) is given by (Fig. 10b):
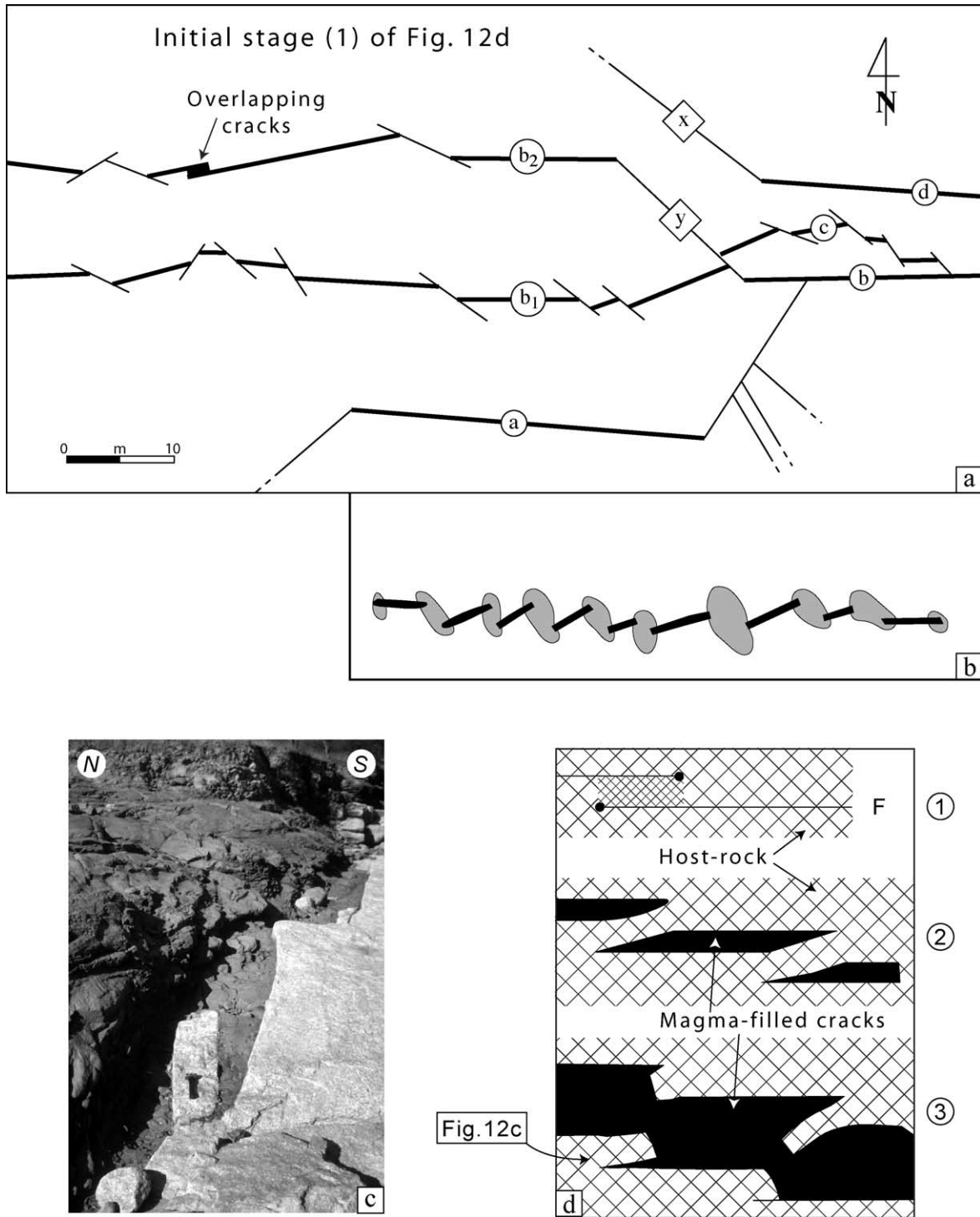
Fig. 12. Examples of segmented Karoo dykes in the N110°/ODS (Shashe Dam site). (a) Initial 2D arrangement of fractures prior to dyke emplacement (final stage in Fig. 9c). 'a, b, c, and d' are inherited en relais fractures (major dyke segments); 'x, y' structures and thin black lines are oblique dyke segments initiated as either basement fractures (long segments) or newly formed tensile zones (short segments interpreted on sketch of (b)). (b) Growth model of linked dyke segments (in black) by increasing tensile failure zones (in grey) at dyke terminations (modified from Rogers and Bird, 1987). (c) Nearly detached slab of country rocks on the southern wall of the 20-m-wide mafic dyke named 'b2' in (a). The hammer on the rotated host-rock block is ∼30 cm long. (d) Diagram showing a possible time sequence for emplacement of magma by dilatation of overlapping en relais cracks (modified from Nicholson and Pollard, 1985). According to this model, the pattern of apophyses at the margins of dyke 'c' (see Fig. 10a1) might result from the failure of a bridge along cross fractures.

$$Wd = W_{max} \times \cos \alpha \qquad (3)$$

The dyke width values applied to the above two studied Karoo swarms give an angle α of 50° in Eq. (3), i.e. close to their angular relationships. It is thus suggested that the fracture/dyke network in the N70°/LDS is dilated at high angle to its walls (as pure extensional structures), whereas those of the N110°/ODS opened obliquely (with an inferred dyke-parallel shear component) to a regional extension that should be roughly oriented at NNW–SSE (Fig. 10b). Assuming that N110°E dykes should have dilated as oblique shear fractures suggests the inherited origin of part of their hosting fracture network, in agreement with additional criteria presented below.

5.3. Inherited and dyke-induced fractures

Whether dykes occupy pre-existing fractures or generate their own fractures is a long-standing debate (Delaney et al., 1986); further emphasized when host-rocks belong to a crystalline basement that recorded a polyphase brittle–ductile history, as for the Archaean rocks in NE Botswana. Discrimination between dyke-generated and inherited fractures has been made here by comparing the fracture abundance close to a given dyke and regional fracture abundance in both basement and sedimentary host-rocks.

In the Permo-Jurassic grit/shale alternations of the Thune section, the only clear deformation related to Karoo dyke injection is curved anastomosing joints, developed a few metres away from dyke margins.

Identification of Karoo dyke-induced brittle structures in highly deformed metamorphic basement terranes (Shashe area) is more difficult. But supportive evidence is locally documented in Francistown quarry (Figs. 2a and 11), where a narrow Karoo (dated) dyke (Le Gall et al., 2002) cuts across Archaean tonalite. The host-rock is intensely disrupted by a dense network of brittle joints, parallel to the dyke margins, that gradually decrease in density 2–3 m apart from the dyke. The symmetrically distributed brittle fractures likely formed as wall-parallel tensile joints in the basement tonalitic rocks during dyke emplacement.

Generally, the Archaean crystalline basement of the Shashe section displays N30–40°E ductile fabrics that are disrupted by close to vertical brittle fractures with a great variety of orientations, including N110°E structures parallel to the ODS trend. Given the various origins of the N110°E fracture surfaces as either strike-slip, reverse fault-related fractures, or extensional joints (mainly deduced from the plunging attitude of striations and sense of displacement), most of them are likely to be inherited basement features formed at some stage of the polyphase tectonic history of the pre-Karoo basement. More convincing evidence for occurrence of pre-existing N110°E basement fabrics, and their role on Karoo dyke orientation, comes from the Shashe Moocke and Borolong areas (Fig. 3a). These two zones, 1–2 km wide each, enclose a dense array of vertical fractures

that are continuous for tens of metres with a constant azimuth of N100–110°E. Their frequency commonly exceeds one fracture per metre. The restricted spatial distribution of this joint/fracture network within segment II, i.e. where basement dykes strictly occur (Fig. 3c), suggests causal links with the Proterozoic dyking process. A quite similar origin is likely for the pattern of dyke-hosting fractures in the adjoining composite segments I and III.

A second network of extensional fractures, expressed as N140°E epidote-filled veins and pegmatitic dykes in granitoid rocks, may also be basement structures that have potentially caused the local segmentation of N110°E Karoo dykes (see Figs. 9c and 12a, and corresponding text below). According to our structural model, the N110°E basement-controlled trend of Karoo dykes in the Shashe area should have rotated 40° (anticlockwise) when crossing through the Permo-Jurassic cover to form perpendicular to regional extension. However, their still persistent N100–110°E orientation along the Thune section (see Fig. 8) probably results from the influence of shallow basement fabrics along the southern flexural margin of the Tuli half-graben.

The fault/fracture system in the N70°/LDS is also believed to be at least partly inherited because of involving basement and Jurassic dykes also (see Fig. 2) (Jourdan et al., 2004b).

5.4. Dyke segmentation

Field relations between highly segmented dykes and basement fabrics in the Shashe Dam site provide important constraints on both dyke segmentation mechanisms and relative ages of fracturing and dyke intrusion. Dilational emplacement of dykes in brittle fractures might have first proceeded by filling of a set of unconnected en relais cracks striking at N80–110°E, the inherited or newly formed origin of which is not firmly defined (Fig. 12a). However, the occurrence of joint fractures, with a similar range of azimuth at N80–110°E, within the gneiss host-rocks, either close to or at a distance from dyke margins, suggests that most of them originate as Proterozoic structures. As such, the sense of shearing (probably right-lateral in the present case) indicated by their dextral en relais arrangement is not relevant to the way fractures later dilate during Karoo dyke emplacement. This sense of shearing is opposite to the component of sinistral shear-sense compatible with the inferred NNW–SSE direction of Karoo extension (see above). The low-angle bayonet-like apophyses occurring with a dominant asymmetry along a number of dyke margins (dyke 'c' in Fig. 10a1, for example) have been used elsewhere as kinematic indicators (Hanmer et al., 1997) and, in the present case, they should indicate a dextral shear-sense. However, quite similar dyke geometry could be obtained from broken host-rock bridges at an offset in dyke (Fig. 12c and d) (Nicholson and Pollard, 1985), whatever the conditions of dyke/fracture opening were.

The linkage of en relais dyke segments occurs via N120–

Table 2
Compiled dyke width data from continental and oceanic ridge settings

Tectono-magmatic setting	Age	Mean dyke width (m)	Reference
BTIP			
Skye	Paleocene	0.6	Walker (1993)
Mull	Paleocene	1.2	Jolly and Sanderson (1995)
Iceland Rifted Zone	Quaternary	<2.0	Gudmundsson (1990a)
	Tertiary	4.0	Gudmundsson (1990a)
Central Atlantic Ridge	Present	1.0	Karson et al. (1999)
Hawai	Present	0.7	Walker (1987)
Mid-Oceanic Ridge	Num. model	$0.2 < W < 3.0$	Head et al. (1996)
Oman Ophiolite	Permo-Triassic	<1.0	Lippard et al. (1986)
Giant Okavango DS	Middle Jurassic	18	This work
Mc Kenzie DS (world's greatest DS)			
Baranga		<30	Anderson and Diehl (1982)
Carlton	Archaean	<15	Chandler (1986)
Duluth		4	Motamedi (1984)

140°E oblique dyke segments possibly initiated in two different ways as a function of the initial dyke spacing. When separation of two adjoining (generally underlapping) N80–110°E dykes is small compared with dyke lengths, tensile failure zones developed at the tip of the propagating cracks (Fig. 12b), in a way predicted by the model of Olson and Pollard (1991). These may have later interacted and coalesced into a single tensile fracture zone, lying at high angle to the dyke trend (Rogers and Bird, 1987). Subsequent infilling with magma leads to the final segmented dyke network (Fig. 12a). Inversely, when dyke separation is greater, mechanical interaction between adjacent crack tips is unlikely. In this case, their connection might have been governed by inherited N120–140°E fractures (X and Y in Fig. 12a) that dilated obliquely with regard to the inferred extension.

6. Discussion and conclusions

Structural analysis of the Okavango (N110°E) and the Limpopo (N70°E) dyke swarms in NE Botswana provides new insights about: (1) the internal organisation of giant mafic dyke swarms; and (2) the structural framework during the emplacement of magma in the northern part of the Karoo LIP. The most significant results of this study come from the Shashe section that intersects the densest dyke zone of the N110°/ODS at high angle. More than 420 dykes recorded from ground magnetics allow us to quantify the dyke population, whereas structural features of the crystalline country rocks help to constrain the role of pre-existing basement fabric on the emplacement of Karoo dykes.

Quantitative results obtained from Karoo dyke geometry in the N110°/ODS do not conform to the properties usually displayed by dykes in other giant mafic swarms. The low frequency of narrow dykes (<5.0 m), when compared with the thickest dykes (16–70 m), is a real feature that still remains to be explained in terms of either mechanical conditions of emplacement, pre-dyke fracture network, or

nature of the magma. The structural significance of the 16–17 m mean dyke width, which is much greater than the 5–10 m considered as typical average dyke thickness for giant dyke swarms (Table 2) (Ernst et al., 1995), is also questionable. The narrowing of N110°E dykes, from 16–17 m in basement host-rocks to 1.3 m into the overlying Permo-Jurassic cover, is rather assigned to the coexistence (Tuli half-graben) or absence (Shashe basement area) of normal faulting with extension accommodated by dyke intrusion, instead of being due to a decrease of magma pressure at higher structural levels. In the Shashe area, dyke-driven dilation is calculated at 7295 m (12%) throughout the 60-km-long highest density dyke zone of the N110°/ODS. On the other hand, the change of Karoo dyke widths from 17 m in the N110°/ODS to 27 m in the N70°/LDS possibly relates to regional principal stresses at the time of dyke emplacement. The N70°E-trending fracture network is assumed to have been favourably oriented (perpendicular to the NNW–SSE extension) for opening as pure tensile fractures with a maximum dilation, whilst under such stress conditions, N110°E dykes should have dilated as oblique shear fractures recording a smaller amount of dilation. It is therefore concluded that: (1) part of the N110°E fracture pattern is inherited and possibly linked to a previous (Proterozoic) dyke intrusion event; and (2) the main controlling factor for the constant N110°E trend of the ODS over more than 1500 km is a major pre-existing basement brittle fabric rather than the orientation of the applied stress field.

The 2D map-view of the 1500-km-long N110°/ODS varies along-strike on regional aeromagnetic maps with a gradual westerly narrowing of the high density dyke zone from 60 km in the Francistown area to 53 and 45 km in the Maun and Ngami areas, respectively (Fig. 13a). It is suggested that dyke-driven extension decreases abruptly westwards (Table 3) from 7295 m (12%) along the Shashe section to 1384 m (2.6%) along the Maun section (400 km to the W) and 1160 m along the Ngami section (200 km further W) (Fig. 13), if we assume that most of the dyke

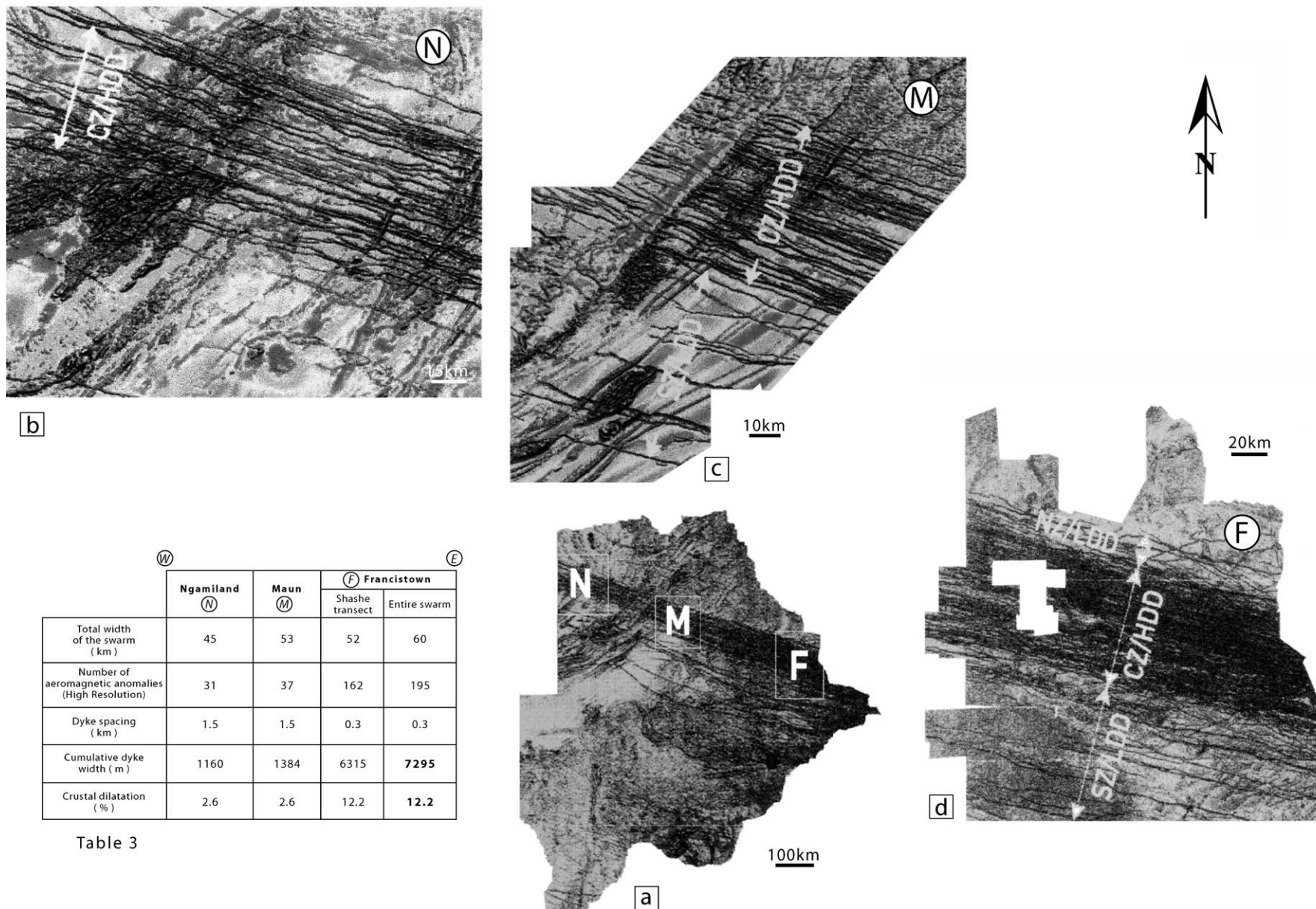|	Ngamiland (N)	Maun (M)	Francistown (F)	
			Shashe transect	Entire swarm
Total width of the swarm (km)	45	53	52	60
Number of aeromagnetic anomalies (High Resolution)	31	37	162	195
Dyke spacing (km)	1.5	1.5	0.3	0.3
Cumulative dyke width (m)	1160	1384	6315	**7295**
Crustal dilatation (%)	2.6	2.6	12.2	**12.2**

Table 3

Fig. 13. Aeromagnetic dataset of NE Botswana (from Tshoso, 2003, modified). (a) Low-resolution aeromagnetic map showing the trace of the N110/ODS. Rectangles are regions covered with high-resolution aeromagnetic data. F, Francistown (study area), M, Maun, N, Ngami. (b)–(d) High-resolution aeromagnetic maps of Ngami (b), Maun (c) and Francistown (d) areas. CZ, NZ, SZ, Central, Northern and Southern zones; HDD, high dyke density.

Table 3
Along-strike variations of the width and dyke-induced extension in the high dyke density zone of the ~1500-km-long Okavango dyke swarm (from aeromagnetic dataset of Tshoso (2003) calibrated using the Shashe section)

	Ngamiland (N)	Maun (M)	(F) Francistown	
			Shashe transect	Entire swarm
Total width of the swarm (km)	45	53	52	60
Number of aeromagnetic anomalies (high resolution)	31	37	162	195
Dyke spacing (km)	1.5	1.5	0.3	0.3
Cumulative dyke width (m)	1160	1384	6315	7295
Crustal dilatation (%)	2.6	2.6	12.2	12.2

parameters measured in the Shashe reference section, e.g. the ratio of Proterozoic/Karoo dykes (~1/6) and the average Karoo dyke thickness (17 m), remain constant along-strike. Such a change in the lateral distribution of dykes in the N110°/ODS, coupled with the lack of map-scale deflection of the swarm trend around magma chambers at depth, suggests that Karoo mafic dykes propagated laterally westwards, away from the Nuanetsi source region (Fig. 14b), instead of being injected vertically from deep-seated linear magmatic ridges. The model of lateral flow of Karoo magma is also supported by anisotropy of magnetic susceptibility data that show a transition from predomi-nantly vertical (Tuli basin) to horizontal (Shashe area) magma flow with increasing distance from the Nuanetsi focal point (Fig. 14b) (Tshoso, 2003), in agreement with the mantle plume hypothesis (Campbell and Griffiths, 1990; Cox, 1992). However, since the N110°/ODS and N70°/LDS

in NE Botswana (this study), as well as the Lebombo (NS), Olifants River (N20°E) and Limpopo (N70°E) dyke swarms seemingly radiating from the Nuanetsi region (Fig. 14b), are polyphase intrusive complexes including both Karoo and Precambrian dykes (Marsh, 2002; Jourdan et al., 2004b) they must follow pre-existing crustal structures extending close to Archaean craton margins (Fig. 14a) (Hutchins and Reeves, 1980). Whatever be the origin of the associated thermal perturbation in the upper mantle, either related to a plume/flat subduction system (Dalziel et al., 2000) or incubation processes as proposed elsewhere (Anderson, 1987), the upward migration of magma through the upper crust of the Karoo LIP should have occurred via vertical conduits at the intersection of deeply rooted basement discontinuities (Cox et al., 1965) that later fed the inherited fault-fracture network laterally (Fig. 14a). Assuming the inherited and polyphase origin of the fracture network
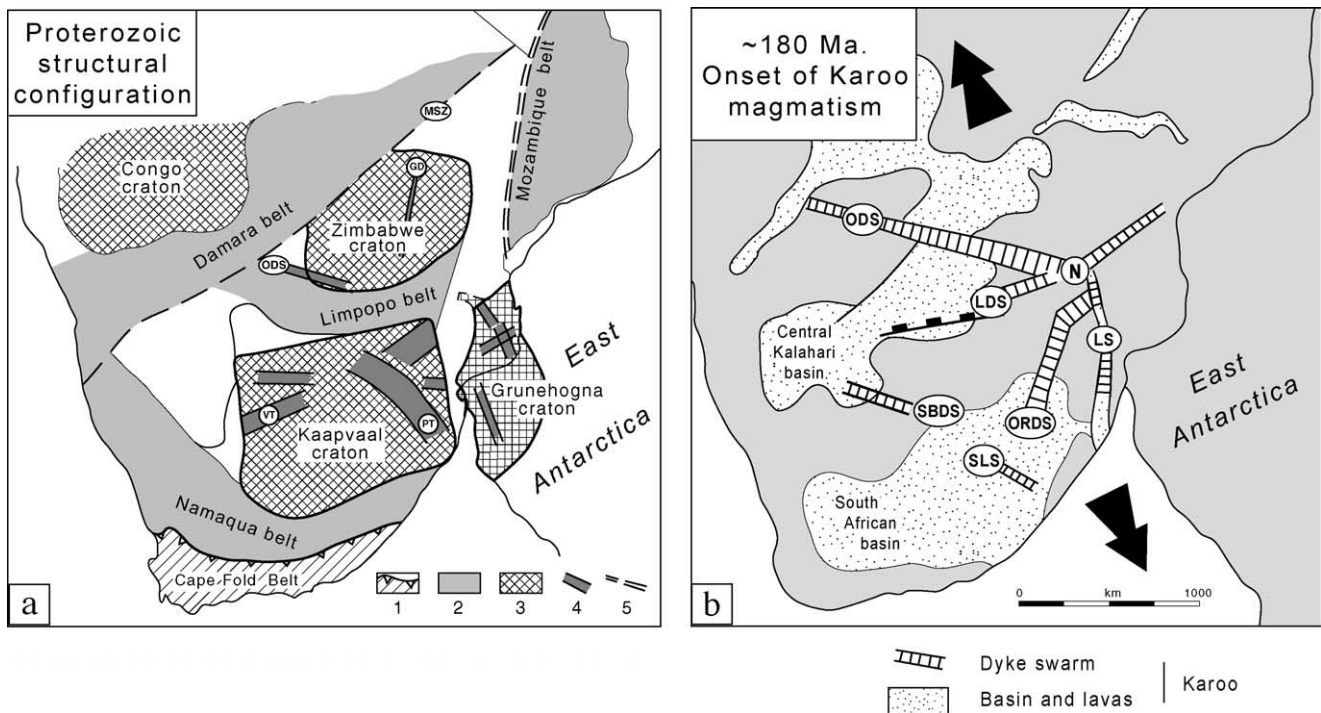

Fig. 14. Major Precambrian and Karoo structural features of West Gondwana. (a) Basement boundaries in southern Africa. (1) Palaeozoic belt; (2) Proterozoic belts; (3) Craton; (4) Dyke swarms; (5) Suture lines. GD, Great Dyke; MSZ, Magogaphate shear zone; PT, Pongola rift trend; ODS, Okavango (proto) dyke swarm; VT, Venterdorp rift trend. (b) Karoo tectono-magmatic framework of southern Africa at the onset of the Middle Jurassic magmatic activity. Constraints in the direction of extension (black arrow) are limited (mainly from our data on NE Botswana Karoo dykes). Same captions as in Fig. 1b.

hosting mafic dykes in the northern Karoo LIP implies that the final radiating arrangement of giant dyke swarms does not constitute unequivocal proof for the existence of a mantle plume. The structural interpretation of the Karoo triple junction-like dyke pattern as a result of radial stress above a plume head, in agreement with the theoretical models of Fahrig (1987) and Ernst and Buchan (1997), is thus considered in the present work as an over-simplification. But further detailed structural works, similar to those discussed here about the Okavango mafic dyke swarm, should be applied to the other giant dyke arms of the triple junction-like system as a prerequisite for any kinematic model of the Karoo LIP.

Acknowledgements

References

Aldiss, D.T., 1981. Tsetsebjwe, 1:250,000 sheet 2228A, Geological Survey of Botswana.

Aldiss, D.T., 1982. Semolale, 1:250,000 sheet 2128D, Geological Survey of Botswana.

Aldiss, D.T., 1986. Shashe, 1:250,000 sheet 2127A, Geological Survey of Botswana.

Anderson, D.L., 1987. Global mapping of the uppermantle by surface wave tomography, composition, structure and dynamics of the lithosphere asthenosphere system. In: Fuchs, K., Froidevaux, C. (Eds.), Geodynamic Series, vol. 16. American Geophysical Union, Washington, DC, p. 327.

Anderson, T.D., Diehl, J.F., 1982. Magnetic Investigations of the Baraga Country Diabase, Michigan, Abstract, Proceedings, 28th Annual Institute on Lake Superior Geology, International Falls, Minnesota, USA 1982, p. 3.

Baer, G., Beyth, M., 1990. A mechanism of dyke segmentation in fractured host rock. In: Parker, A.J., Rickwood, P.C., Tucker, D.H. (Eds.), Mafic Dykes and Emplacement Mechanims. Balkema, Rotterdam, pp. 3–11.

Baer, G., Beyth, M., Reches, Z., 1994. Dikes emplaced into fractured basement, Timna Igneous Complex, Israel. Journal of Geophysical Research 99, 24039–24050.

Bennett, J.D., 1969. Magogaphate, 1:250,000 sheet 2128C, Geological Survey of Botswana.

Brewer, T.S., Hergt, J.M., Hawkesworth, C.J., Rex, D., Storey, B.C., 1992. Coats Land dolerites and the generation of Antarctic continental flood basalts. In: Storey, B.C., Alabaster, T., Pankhurst, R.J. (Eds.), Magmatism and the Causes of Continental Break-up. Geological Society of London, Special Publication 68, 185–208.

Burke, K., Dewey, J.F., 1972. Plume generated triple junctions. Key indicators in applying plate tectonics to old rocks. Journal of Geology 81, 403–433.

Callot, J.P., Grigné, C., Geoffroy, L., Brun, J.P., 2001. Development of volcanic passive margins: two-dimensional laboratory models. Tectonics 23, 148–159.

Campbell, I.H., Griffiths, R.W., 1990. Implications of mantle plume structure for the evolution of flood basalts. Earth and Planetary Science Letters 99, 79–93.

Chandler, V.W., 1986. Interpretation of Precambrian geology in Minnesota using low-altitude, high-resolution aeromagnetic data. In: Hinze, W.J. (Ed.), The Utility of Regional Gravimetry and Magnetic Anomaly Maps. Society of Exploration Geophysicists, Tulsa, USA, pp. 375–391.

Childs, C., Walsh, J.J., Watterson, J., 1990. A method for estimation of the density of fault displacements below the limit of seismic resolution in reservoir formations. In: Buller, A.T. (Ed.), North Sea Oil and Gas Reservoir II. The Norwegian Institute of Technology/Graham & Trotman, London, pp. 309–318.

Cladouhos, T.T., Marrett, R., 1996. Are fault growth and linkage consistent with power-law distributions of fault lengths? Journal of Structural Geology 18, 281–293.

Clark, G.C., Machacha, T.P., 1976. Baines Drift, 1:250,000 sheet 2228B, Geological Survey of Botswana.

Cox, K.G., 1992. Karoo igneous activity, and the early stages of the break-up of Gondwanaland. In: Storey, B.C., Alabaster, T., Pankhurst, R.J. Magmatism and the Causes of Continental Break-up. Geological Society of London, Special Publication 68, 137–148.

Cox, K.G., Jonhson, R.L., Monkman, L.J., Stillman, C.J., Vail, J.R., Wood, D.N., 1965. The geology of the Nuanetsi igneous province. Philosophical Transactions Royal Society of London A257, 71–218.

Dalziel, I.W., Lawver, L.A., Murphy, J.B., 2000. Plumes, orogenesis, and supercontinental fragmentation. Earth and Planetary Science Letters 178, 1–11.

Delaney, P.T., Pollard, D.D., Zioney, J.I., McKee, E.H., 1986. Field relations between dikes and joints: emplacement processes and paleostress analysis. Journal of Geophysical Research 91, 4920–4938.

Elburg, M., Goldberg, A., 2000. Age and geochemistry of Karoo dykes from northeast Botswana. Journal of African Earth Sciences 31, 539–554.

Ernst, R.E., Buchan, K.L., 1997. Giant radiating dyke swarms: their use in identifying pre-Mesozoic large igneous provinces and mantle plumes. In: Mahoney, J.J., Coffin, M.F. (Eds.), Large Igneous Provinces: Continental, Oceanic and Planetary Flood Volcanism. AGU Geophysical Monograph, 100, pp. 297–333.

Ernst, R.E., Buchan, K.L., Palmer, H.C., 1995. Giant dyke swarms: characteristics, distribution and geotectonic implications. In: Baer, G., Heimann, A. (Eds.), Physics and Chemistry of Dykes. Balkema, Rotterdam, pp. 3–21.

Fahrig, W.F., 1987. The tectonic settings of continental mafic dyke swarms. In: Halls, H.C., Fahrig, W.F. (Eds.), Mafic Dyke Swarms Special Paper, 34. Geological Association of Canada, pp. 331–348.

Fossen, H., Rornes, A., 1996. Properties of fault populations in the Gullfaks field, northern North Sea. Journal of Structural Geology 18, 179–190.

Gudmundsson, A., 1990a. Emplacement of dikes, sills and crustal magma chambers at divergent plate boundaries. Tectonophysics 176, 257–275.

Gudmundsson, A., 1990b. Dyke emplacement at divergent plate boundaries. In: Parker, A.J., Rickwood, P.C., Tucker, D.H. (Eds.), Mafic Dykes and Emplacement Mechanims. Balkema, Rotterdam, pp. 47–62.

Hanmer, S., Mengel, F., Connelly, J., Van Gool, J., 1997. Significance of crustal-scale shear zones and synkinematic mafic dykes in the Nagssugtoqidian orogen, SW Greenland: a re-examination. Journal of Structural Geology 19, 59–75.

Head, J.W., Wilson, L., Smith, D.K., 1996. Mid-ocean eruptive vent

morphology and substructure: evidence for dike widths, eruption rates, and evolution of eruptions and axial volcanic ridges. Journal of Geophysical Research 101, 28265–28280.

Hutchins, D.G., Reeves, C.V., 1980. Regional geophysical exploration of the Kalahari in Botswana. Tectonophysics 69, 201–220.

Jolly, R.H., Sanderson, D.J., 1995. Variation in the form and distribution of dykes in the Mull swarm, Scotland. Journal of Structural Geology 17, 1543–1557.

Jones, D.L., Duncan, R.A., Briden, J.C., Randall, D.E., MacNiocaill, C., 2001. Age of the Batoka basalts, northern Zimbabwe, and the duration of Karoo Large Igneous Province magmatism. Geochemistry, Geophysics, Geosystems 2, 1–15.

Jourdan, F., Féraud, G., Bertrand, H., Kampunzu, A.B., Tshoso, G., Le Gall, B., Tiercelin, J.J., Capiez, P., 2004a. The Karoo triple junction questioned: evidence from ^{40}Ar/^{39}Ar Jurassic and Proterozoïc ages and geochemistry of the Okavango giant dyke swarm (Botswana). Earth and Planetary Science Letters 222, 989–1006.

Jourdan, F., Féraud, G., Bertrand, H., Kampunzu, A.B., Watkeys, M., Tshoso, G., Le Gall, B., 2004b. New age constraints on the Karoo Large Igneous Province: triple junction and brevity questioned. Goldschmidt Geochemistry Conference, Copenhagen.

Karson, J.A., Klein, E.M., Hurst, S.D., 1999. Internal structure of uppermost fast-spread oceanic crust of the East Pacific Rise exposed at the Hess Deep Rift: results from Alvin, Argo II, and DSI 120 investigations. EOS Transactions AGU (Abstract), F983–F984.

Le Gall, B., Thsoso, G., Jourdan, F., Féraud, G., Bertrand, H., Tiercelin, J.J., Kampunzu, A.B., Modisi, M., Dyment, J., Maia, M., 2002. ^{40}Ar–^{39}Ar geochronology and structural data from the giant Okavango and related mafic dyke swarms, Karoo igneous province, N Botswana. Earth and Planetary Science Letters 202, 595–606.

Lippard, S.J., Shelton, A.W., Gass, I. (Eds.), 1986. The Ophiolite of Northern Oman. Blackwell, Oxford. 178pp.

Marsh, J., 2002. Discussion 'The geophysical mapping of Mesozoic dyke swarms in southern Africa and their origin in the disruption of Gondwana'. Journal of African Earth Sciences 35, 525–527.

McCourt, S., Armstrong, R.A., 1998. SHRIMP U–Pb zircon geochronology of granites from the Central Zone, Limpopo belt, southern Africa: implications for the age of the Limpopo Orogeny. South Africa Geological Society 101, 329–338.

Motamedi, S., 1984. The Keweenawan lavas in the City of Duluth. Unpublished MS Thesis. University of Minessota, 140pp.

Nicholson, R., Pollard, D.D., 1985. Dilatation and linkage of echelon cracks. Journal of Structural Geology 7, 583–590.

Olson, J., Pollard, D.D., 1991. The initiation and growth of en echelon veins. Journal of Structural Geology 13, 595–608.

Reeves, C.V., 2000. The geophysical mapping of Mesozoic dyke swarms in southern Africa and their origin in the disruption of Gondwana. Journal of African Earth Sciences 30, 499–513.

Rogers, R.D., Bird, D.K., 1987. Fracture propagation with dike emplacement at the Skaergaard intrusion, East Greenland. Journal of Structural Geology 9, 71–86.

Scholz, C.H., Cowie, P.A., 1990. Determination of total strain from faulting using slip-measurements. Nature 346, 837–839.

Tshoso, G., 2003. Structure, chronologie et mode de mise en place du système de dykes géants de l'Okavango, Nord Botswana. Une approche pluridisciplinaire. Published PhD Thesis. Brest University, 186pp.

Wada, Y., 1994. On the relationship between dike width and magma viscosity. Journal of Geophysical Research 99 (B9), 17743–17755.

Walker, G.P., 1987. The dike complex of Koolau volcano, Oahu: internal structure of a Hawaiian rift zone. US Geological Survey, Professional Paper 1350, 961–993.

Walker, G.P., 1993. Re-evaluation of inclined intrusive sheets and dykes in the Cuillins volcano, Isle of Skye. In: Prichard, H.M., Alabaster, T., Harris, N.B., Neary, C.R. (Eds.), Magmatic Processes and Plate Tectonics Special Publication, 76. Geological Society of London, pp. 489–497.

White, R.S., 1992. Magmatism during and after continental break-up. In: Storey, B.C., Alabaster, T., Pankhurst, R.J. Magmatism and the Causes of Continental Break-up. Geological Society of London, Special Publication 68, 1–16.

White, R.S., McKenzie, D.P., 1989. Magmatism at rift zones: the generation of volcanic continental margins and flood basalts. Journal of Geophysical Research 94, 7685–7729.